Available online at www.sciencedirect.com
ScienceDirect
Journal of Photochemistry and Photobiology A: Chemistry 195 (2008) 47–53
Journal of Photochemistry and Photobiology A:Chemistry
www.elsevier.com/locate/jphotochem

Direct growth of F-doped TiO_2 particulate thin films with high photocatalytic activity for environmental applications

Guosheng Wu, Aicheng Chen *

Department of Chemistry, Lakehead University, Thunder Bay, Ontario P7B 5E1, Canada

Received 16 June 2007; received in revised form 14 August 2007; accepted 3 September 2007
Available online 7 September 2007

Abstract

Here we report on a novel and facile approach to directly grow F-doped TiO_2 particulate thin films with superb visible light photoelectrical response and high photocatalytic efficiency by oxidizing titanium plates in the presence of H_2O vapor assisted with NaF at relatively low temperatures. The effects of the oxidation temperature and the amount of the NaF coated on the titanium plates on the morphology and the photocatalytic properties of the formed F-doped TiO_2 particulate thin films have been investigated. The formed F-doped TiO_2 particulate thin films show a significant increase in the photocurrent of photoinduced splitting of water into hydrogen and oxygen compared with that of commercial P-25 TiO_2, under irradiation of either UV or visible light. In addition, the photocatalytic activity of the formed F-doped TiO_2 particulate thin films out perform the commercial P-25 TiO_2 for the photodegradation of 4-nitrophenol under UV and visible light irradiation. The approach described in this study can be easily commercialized to fabricate F-doped TiO_2 particulate thin films on a large-scale for very promising environmental applications in the photodegradation of organic pollutants and photoinduced splitting of water into hydrogen, a *green* energy source.

Keywords: TiO_2 thin film; F-doping; Photocatalysis; Splitting of water; Wastewater treatment

1. Introduction

Photocatalysis has gained considerable attention owing to its widespread environmental applications in air purification, water disinfection and hazardous waste remediation in recent years [1–3]. Among various oxide semiconductor photocatalysts, titania (TiO_2) is currently one of the most promising photocatalysts because of its biological and chemical inertness, cost effectiveness and the strong oxidizing power of photogenerated holes. Under UV irradiation, TiO_2 can catalyze many reactions, for instance, alcohol dehydration, photo-Kolbe oxidation of organic acids [4], oxidation of aromatic compounds [5,6], degradation of paint pigments [7], and nitrogen oxide reduction [8]. It is well known that the first step of a heterogeneous photocatalytic process, generation of the electron (e^-)–hole (h^+) pairs, is initiated upon irradiation of photons with energy greater than or equal to the band gap energy of the photocatalyst. The photogenerated electrons and holes can either recombine in the bulk or migrate to the surface to initiate various redox reactions. A high surface area is thus desirable to increase photocatalytic efficiency. To achieve a high surface area, recently tiatnia has been fabricated in the form of different nanostructures such as ordered macroporous particles [9], nanoparticles [10], nanowires [11,12] and nanotubes [13,14] using various methods. The main drawback of TiO_2 is that its band gap lies in the near-UV of the electromagnetic spectrum: 3.2 eV and 3.0 eV for anatase and rutile, respectively. As a result, only UV light can create the electron–hole pairs and initiate the photocatalytic processes. This inherent property of TiO_2 curtails the overall efficiency of sunlight, a renewable energy source, as only about 3–5% of total sunlight can photoactivate titania to generate the charge carriers (electrons and holes) that ultimately can be exploited to promote surface reduction and oxidation processes. One possible approach to overcome this drawback is to red-shift the absorption edge of TiO_2 to wavelengths longer than 400 nm by creating energy levels within the band gap or to shift the conduction band (CB) and/or the valence band (VB) so that visible light can excite electrons. TiO_2-based photocatlysts doped with either anions (e.g. C, N, S, F) [15–19] or cations (Fe^{3+}, Mo^{5+}, Ru^{3+}, etc.) or modified with some metals (Pt, Au, Ag, Cr, V, Mn, Nb) [20–25]

* Corresponding author. Tel.: +1 807 3438318; fax: +1 807 3467775.
E-mail address: aicheng.chen@lakeheadu.ca (A. Chen).

1010-6030/$ – see front matter © 2007 Elsevier B.V. All rights reserved.
doi:10.1016/j.jphotochem.2007.09.005

have been widely investigated in order to have their absorption edge red-shifted to lower energies (longer wavelengths) and to enhance the photocatalytic efficiency of photoassisted surface redox reactions.

In addition, it is known that semiconductor particles dispersed as a suspension behave as shorted circuited microelectrodes under band gap excitation and thus promote oxidation and reduction on the same particle. For example, complete mineralization of phenolic compounds is achieved with the excitation of suspended anatase TiO_2. However, there are two major disadvantages of such a system: (i) the high degree of recombination of the photogenerated charge carriers and (ii) the requirement of separation and recycling of the TiO_2 fine particles by filtration. A process that avoids the filtration step would be of great practical benefit in the photochemical treatment of wastewater. On the other hand, the semiconductor particulate films provide a convenient way of manipulating the photocatalytic reaction by electrochemical methods. The recombination between the photogenerated charge carriers can be effectively suppressed by applying an external anodic bias [26].

Moreover, TiO_2 thin films have received increasing attention in recent years due to the large-scale commercialization of self-cleaning glazing products which use titania as a photocatalyst to provide the self-cleaning properties. A number of techniques have been developed for depositing TiO_2 thin films [27–29]. Titanium is the world's fourth most abundant metal (exceeded only by aluminum, iron, and magnesium) and the ninth most abundant element. It is also widely used as a substrate in fabricating Dimensionally Stable Anodes (DSA®) because of its excellent corrosion–resistance and relative low cost. Utilizing titanium as the substrate for titania film growth opens up many potential applications including self-cleaning/sterilizing hospital equipment and antimicrobial coatings.

Recently, we studied the direct oxidation of titanium plates to form TiO_2 nanostructures using different oxygen sources such as ethanol, acetaldehyde, acetone, dibutyltin dilaurate, formic acid and water vapor [30]. The water contact angle measurements reveal that the wetting properties of the formed TiO_2-nanostructured films are dictated by their structure, varying from a hydrophilic surface to a highly hydrophobic surface. However, the oxidation process has to be carried out at high temperatures (e.g. 850 °C), resulting in the formation of rutile TiO_2 nanostructures. Although rutile TiO_2 possesses a high refractive index and has extensive optical applications, anatase is more desirable for photocatalysis. In this study, we report on a novel and facile approach to directly grow F-doped TiO_2 particulate thin films with high visible light photoelectrical response and photocatalytic efficiency by oxidizing titanium substrate in the presence of H_2O vapor assisted with NaF at relatively low temperatures (e.g. 600 °C).

2. Experimental

2.1. Catalyst preparation and characterization

Titanium plates of 8.0 mm × 12.5 mm × 1.0 mm were first degreased using acetone, then washed with distilled water, etched in 18% HCl at 85 °C for 15 min to remove the oxide layer on the surface, then completely washed with distilled water and finally dried in a vacuum oven at 40 °C. The growth of the TiO_2 thin films was carried out in a horizontal tube furnace equipped with a quartz tube (diameter 3.5 cm, length 70 cm). The setup and method used here are similar to chemical vapor deposition (CVD). Prior to heating, the pretreated Ti plates were coated by 500 μl of NaF solution with concentrations varying from 0.0 M to 0.2 M, then dried in a vacuum oven at 40 °C and finally placed into the center of the quartz tube. The system was purged using ultrapure argon (99.9995%) at a flow rate of 200 standard cubic centimeters per minutes (sccm) for 4 h. Then the argon carrier was switched to pass through heated distilled water (∼90 °C) in order to introduce H_2O vapor into the system. The system was heated to pre-selected temperatures and kept constant for 3 h. Finally, the system was cooled to room temperature with a continuous purge of a pure argon stream. The as-synthesized samples were dipped into distilled water for 24 h, washed several times with distilled water, and then dried in a vacuum oven at 40 °C. The synthesized TiO_2 thin films were characterized by X-ray diffraction (XRD) (Philips PW 1050-3710 Diffractometer with Cu Kα radiation) and scanning electron microscopy (SEM) (JEOL JSM 5900LV).

2.2. Activity test

The photocatalytic activity of the synthesized F-doped TiO_2 particulate thin films was investigated using the photoinduced splitting of water into hydrogen and oxygen, which has been one of the most significant targets of semiconductor photocatalysis, having promising applications in converting solar energy into chemical energy. The photoinduced current of the F-doped TiO_2 particulate thin films was measured in a 0.5 M Na_2SO_4 electrolyte using a three-electrode configuration with a Pt coil counter electrode and a saturated Ag/AgCl reference electrode (PGZ 301, Radiometer analytical). The UV source was CureSpot 50 (ADAC systems), the wavelength range was from 280 nm to 450 nm. The light from the source was guided through a fiber and projected on the surface of samples. The measured light irradiance was around 2 mW/cm^2. For visible light irradiance, the source light was passed through an optical filter (Edmund Optics), cutting off wavelengths below 420 nm; and the intensity of the remaining visible light available in this study was ∼0.015 mW/cm^2.

The photocatalytic activity of the synthesized F-doped TiO_2 particulate thin films was further tested using 4-nitrophenol as a model pollutant. Nitrophenols are among the most common organics of toxic persistent pollutants in industrial and agricultural wastewater. They are considered to be hazardous waste and priority toxic pollutants by the U.S. Environmental Protection Agency. Purification of wastewater polluted with 4-nitrophenol is very difficult as the presence of a nitro group in the aromatic ring enhances the stability of 4-nitrophenol in chemical and biological degradation. 0.5 M NaOH was employed as the supporting electrolyte. We started testing with an initial concentration of 7.5×10^{-5} M 4-nitrophenol; the change of the concentration of 4-nitrophenol in the course of the photodegra-

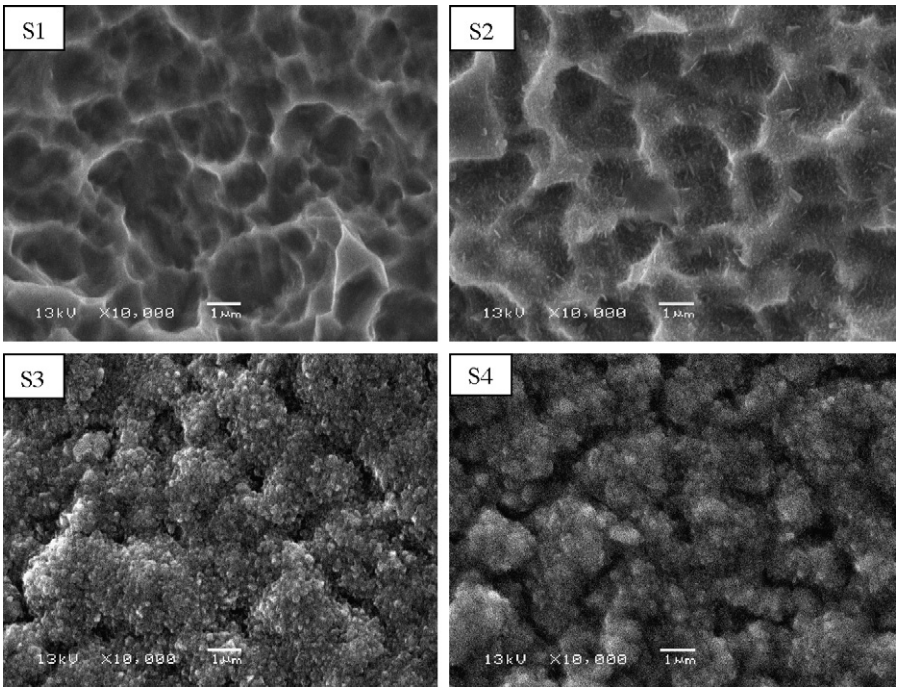

Fig. 1. SEM images of the thin films grown on the titanium plates in the presence of water vapor assisted with NaF at different temperatures: (S1) 500 °C; (S2) 550 °C; (S3) 600 °C; and (S4) 650 °C.

dation was monitored by an *in situ* UV–vis spectroscopy (EPP StellarNet Inc.). For comparison, a commercially available TiO_2 powder (Degussa P-25) was used to prepare thin particulate films on titanium plate and was also tested in this study.

3. Results and discussion

3.1. Effect of temperature

Fig. 1 shows the SEM images of the thin films formed on the titanium plates in the presence of water vapor assisted with NaF at different temperatures: (S1) 500 °C; (S2) 550 °C; (S3) 600 °C; and (S4) 650 °C. All the titanium plates were etched, coated with 500 μL of 0.1 M NaF and dried before the high temperature oxidation treatment. At the lowest temperature of 500 °C, as shown in S1, the surface is still rough and very similar to the chemically etched titanium substrate before the thermal oxidation. Increasing the temperature to 550 °C (S2), although we can still see the profile resulting from the chemical etching, the surface becomes less rough and a small number of particles are formed on the surface. Further increasing the temperature to 600 °C (S3), the etched profile disappears; a nanoparticulate film forms on the Ti substrate. The diameter of these particles is around 100 nm. At 650 °C (S4), the particle size further increases to about 150 nm.

The corresponding XRD patterns of S1–S4 are shown in Fig. 2. The peaks marked with a star derive from the Ti substrate. The intensity of the Ti peaks dramatically decreases when the temperature increases from 500 °C to 650 °C, showing that the thickness of the formed TiO_2 nanoparticulate film significantly increases. This is consistent with the SEM images shown in Fig. 1. The diffraction peaks, (1 1 0), (1 0 1), (1 1 1), (2 1 0), (2 1 1), (2 2 0), (3 1 0) and (3 0 1) are indexed to those of the tetragonal rutile TiO_2 phase; while the diffraction peaks, (1 1 2), (1 0 5), and (2 0 4) are attributed to those of the tetragonal anatase TiO_2 phase. The absence of the diffraction peak (1 1 0) and the presence of the strong diffraction peak (1 1 2) for S1 and S2 show that anatase TiO_2 was formed at the lower temperatures of 500 °C and 550 °C. All the diffraction peaks arising from anatase and rutile TiO_2 that are observed for S3 and S4 demonstrate that the TiO_2 nanoparticulate films formed at the higher temperatures 600 °C and 650 °C possess a mixture of anatase and rutile. The much stronger intensity of peak (1 1 0) shown

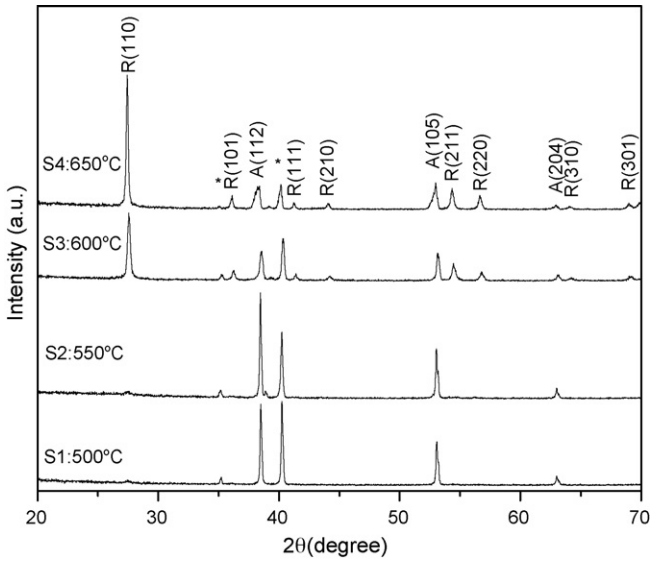

Fig. 2. XRD patterns of S1, S2, S3 and S4.

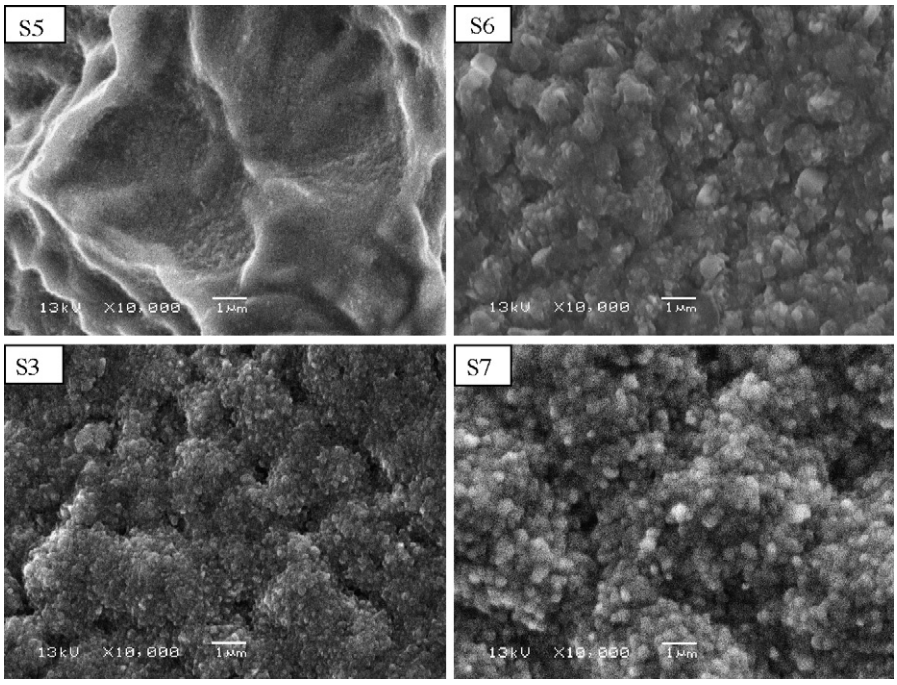

Fig. 3. SEM images of the films grown at 600 °C in the presence of water vapor assisted with different amounts of NaF coated on the titanium plates: (S5) 0 μmol; (S6) 25 μmol; (S3) 50 μmol; and (S7) 100 μmol.

from S3 to S4 indicates that the portion of the rutile phase also increases in the formed TiO_2 nanoparticulate films as the temperature increases to 600 °C and 650 °C. In addition, no NaF diffraction peaks were observed for all the prepared samples, indicating that all unreacted NaF was completely removed from the surface during the 24 h immersion in distilled water.

3.2. Influence of the NaF

Given the above experimental results, 600 °C was chosen to study the effect of the coated NaF amount on the formation of the TiO_2 nanoparticulate films. Fig. 3 presents the SEM images of the thin films directly grown on the titanium plates at 600 °C in the presence of water vapor with different amounts of NaF: (S5) 0 μmol; (S6) 25 μmol; (S3) 50 μmol; and (S7) 100 μmol. The chemically etched profile can be still seen in S5; there is no obvious change of the surface before and after the oxidation process in the absence of the coated NaF. This is consistent with our previous study showing that there is no obvious change of the Ti surface before and after the oxidation process at 650 °C in the presence of H_2O vapor but in the absence of NaF [30]. As shown in S6, some small grains form on the Ti substrate when 25 μmol of NaF is coated on the substrate. Increasing the coated NaF to 50 μmol, the formed grains become smaller (S3); and the grains turn to nearly spheres with 100 μmol of coated NaF (S7).

Fig. 4 presents the corresponding XRD patterns of the four samples shown in Fig. 3. The four samples were prepared under the same experimental conditions except for the different amounts of NaF coated on the Ti substrate. Comparison of the four XRD patterns shows that: (i) both anatase and rutile phase TiO_2 coexist in these samples; (ii) the thickness of the formed TiO_2 thin films increases with the increment of the coated NaF from 0 μmol to 50 μmol; (iii) there is no obvious change of the TiO_2 film thickness when we further increased the coated NaF from 50 μmol to 100 μmol; and (iv) no NaF diffraction peaks were found in the XRD patterns. To further elucidate the function of the F^- ion, two Ti substrates coated with 100 μmol of NaCl and NaOH, respectively, were thermally treated at 600 °C in the presence of water vapor for 3 h. Their surface morphology is very similar to Fig. 3(S5); no particles were formed on the surface. All the above results indicate that the presence of F^- plays a key role in the formation of the TiO_2 particulate thin films,

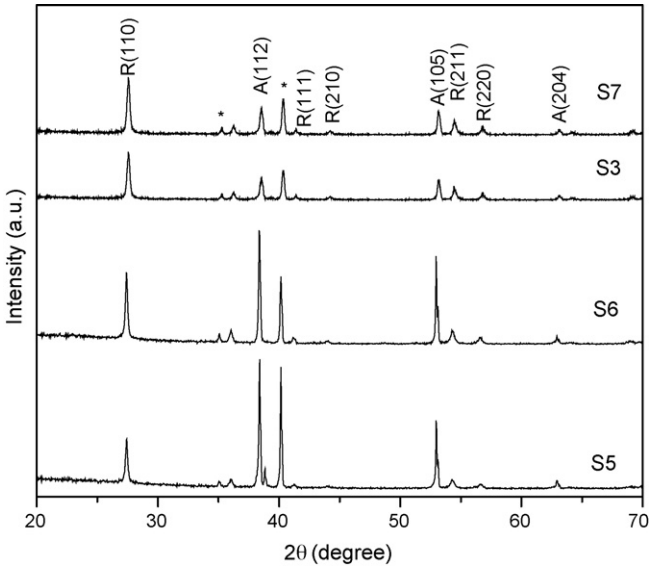

Fig. 4. XRD patterns of S5, S6, S3, and S7.

similar to its role in the formation of TiO_2 nanotubes during anodic oxidation of Ti substrates [13,14,31]. At temperatures higher than 550 °C, Ti reacts with water vapor forming TiO_2

$$Ti + 2H_2O \rightarrow TiO_2 + 2H_2 \quad (1)$$

The formed TiO_2 reacts with the F^- and H^+, producing $[TiF_6]^{2-}$. The formed $[TiF_6]^{2-}$ can also interact with H_2O vapor to form TiO_2

$$TiO_2 + 6F^- + 4H^+ \rightleftharpoons [TiF6]^{2-} + 2H_2O \quad (2)$$

The continuous occurrence of reactions (1) and (2) results in the formation of the TiO_2 particulate thin film.

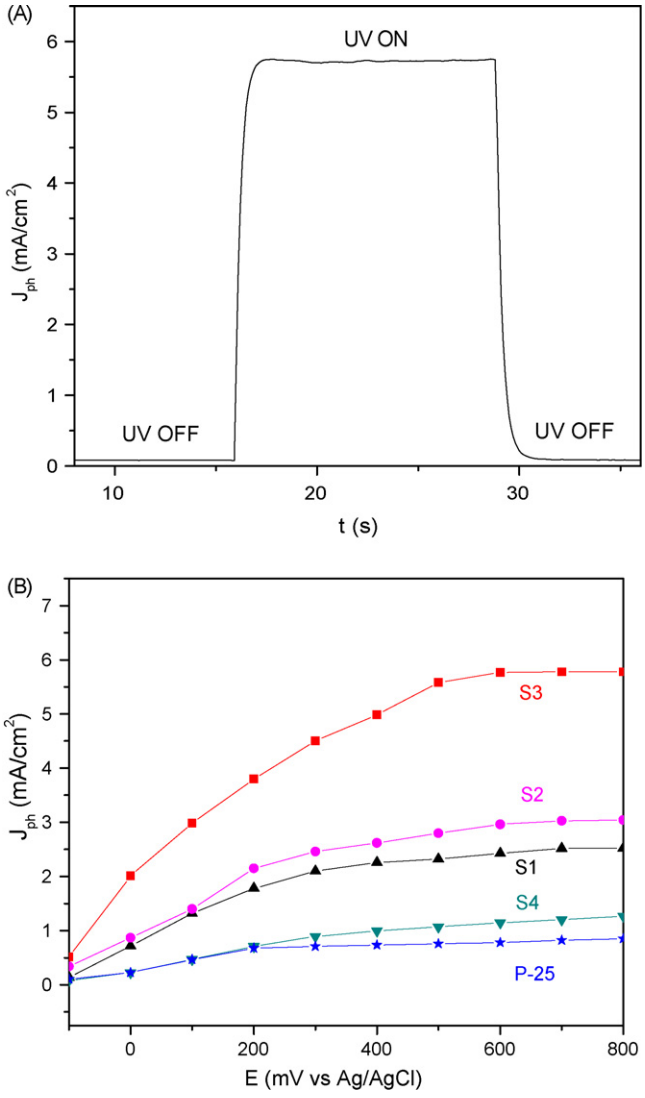

Fig. 5. (A) Photocurrent response of TiO_2 nanofilms prepared using 0.1 M NaF at 600 °C in 0.5 M Na_2SO_4 electrolyte irradiated with UV–visible light. (B) Variation of photocurrent density vs. measured potential for the TiO_2 nanofilms and the P-25 film prepared using 0.1 M NaF at different temperatures in 0.5 M Na_2SO_4 electrolyte irradiated with UV–visible light.

3.3. Photocurrent response

Fig. 5A shows the photocurrent response of S3 (prepared at 600 °C in the presence of water vapor and with 50 μmol of NaF coated on the Ti substrate) at an applied electrode potential of 600 mV versus Ag/AgCl in a 0.5 M Na_2SO_4 solution. In the dark, as expected, the electrochemical current is very low as TiO_2 is a poor electrochemical catalyst for the electrolysis of water. A prompt generation of photocurrent is seen when the electrode is illuminated with UV light. Intensive gas evolution is observed on both the TiO_2 particulate thin film and the Pt counter electrode due to the water splitting reaction. The photocurrent is very high, 5.77 mA/cm^2, although the illuminated UV intensity is relative low, ~2 mW/cm^2. The photocurrent quickly falls to zero once the UV light is switched off.

Fig. 5B presents the j versus E curves for the four TiO_2 thin films (S1–S4) prepared at different temperatures in the presence of water vapor and with 50 μmol of NaF coated on the Ti substrate. For comparison, the j versus E curve for the P-25 particulate film is also included in Fig. 5B. Under the UV illumination, anodic photocurrents are observed for all the thin film electrodes, indicating that all the formed TiO_2 thin films are n-type semiconductors [32]. Fig. 5B shows that: (i) the photocurrents increase with increasing the applied electrode potential from −100 mV to 600 mV versus Ag/AgCl for each sample; and (ii) the photocurrents increase with increasing the oxidation temperature from 500 °C to 600 °C, but dramatically decrease when further increasing the temperature from 600 °C to 650 °C. This is consistent with the SEM and XRD studies shown in Figs. 1 and 2. The TiO_2 thin film formed at the lower temperatures of 500 °C (S1) and 550 °C (S2) has anatase phase, and the thickness of the film is much smaller than that of the TiO_2 films formed at the higher temperatures of 600 °C (S3) and 650 °C (S4). Due to the thicker film plus the particulate structure, the active surface area of S3 and S4 is much higher than that of S1 and S2. As shown in Fig. 2, rutile is the dominative phase in S4. This is why S3 shows the highest photocurrent and S4 exhibits the lowest photocurrent among the four samples. The photocurrent of S3 is 7.4 times higher than that of the P-25 particulate film when an anodic bias of 600 mV is applied. To further study the effect of NaF, Fig. 6 presents the j versus E curves for the photoanodes (S3, S5, S6 and S7) prepared at the same temperature 600 °C in the presence of water vapor but with different amounts of NaF coated on the Ti substrate. Among the four photoanodes, S5, without NaF coated on the Ti plate has the lowest photocurrent; while S3, with 50 μmol of NaF coated on the Ti substrate, exhibits the highest photocurrent.

It has been reported that F-doped TiO_2 induces visible-light-driven photocatalysis [19,33]. We further tested the visible light photoelectrical response of the formed TiO_2 films. Fig. 7 shows a comparison of the photocurrent density versus applied potential curves for the TiO_2 particulate film (S3) and the P-25 film under visible light irradiation (~0.015 mW/cm^2). As expected, there is no photocurrent response for the P-25 thin film. In contrast, the TiO_2 particulate film (S3) exhibits strong photocurrent response under the visible light irradiation; its photocurrent reaches over 40 μA/cm^2 even under the weak visible light irra-

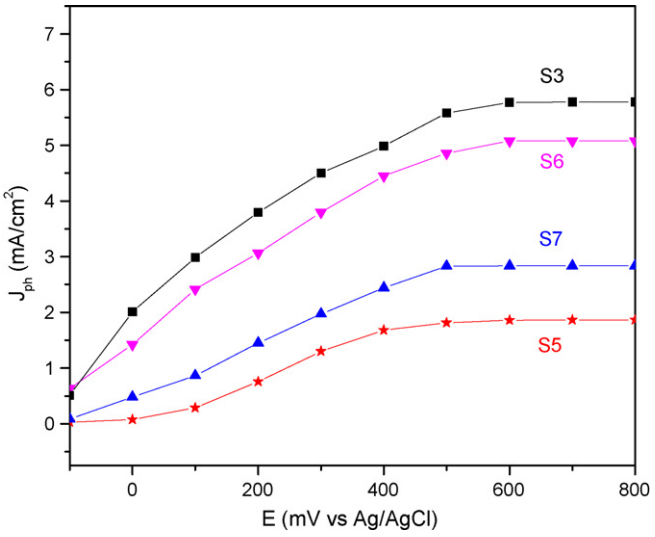

Fig. 6. Variation of photocurrent density vs. measured potential of the TiO_2 nanofilms prepared with different concentrations of NaF at 600 °C.

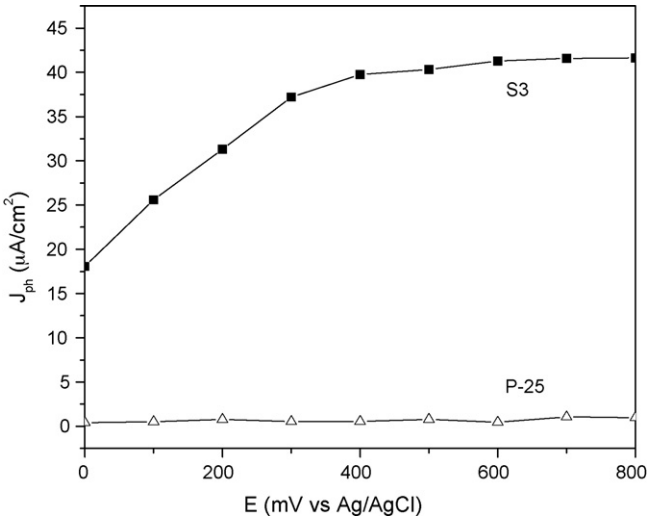

Fig. 7. Variation of photocurrent density vs. measured potential for P-25 film and S3 in 0.5 M Na_2SO_4 electrolyte irradiated with visible light (~0.015 mW/cm^2).

diation (~0.015 mW/cm^2) when the applied anodic bias is over 400 mV. All these results show that F ions are doped into TiO_2 in the course of the formation of the particulate TiO_2 thin film. The strong visible light photocurrent response is due to the formation of Ti^{3+} and oxygen vacancies caused by F^- doping [19,34].

4-Nitrophenol (4-NPh) was used as a model organic pollutant to evaluate the photocatalytic efficiency of the F-doped particu-

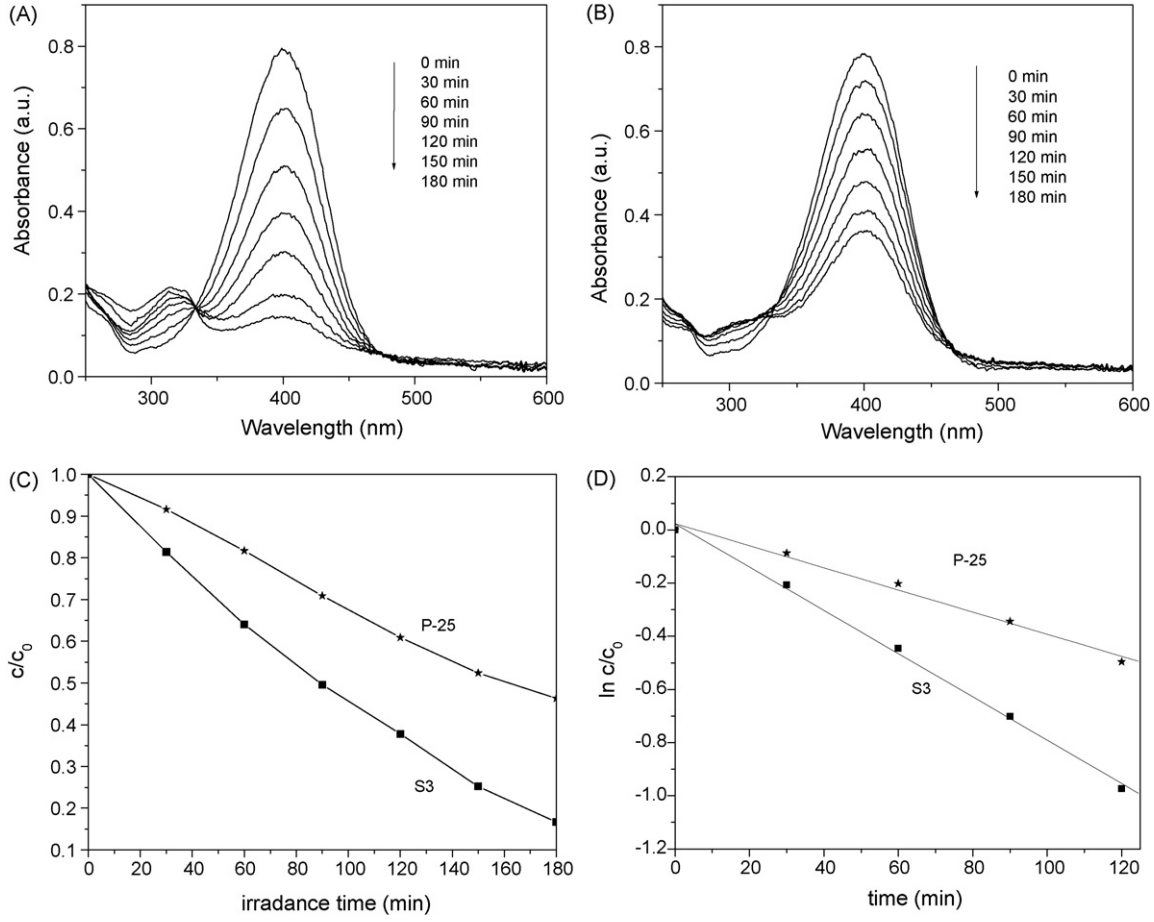

Fig. 8. (A) UV–vis spectra of the F-doped TiO_2 nanofilm (S3) taken during the photoreaction of 0.075 mM 4-nitrophenol based solution; (B) UV–vis spectra of P-25 samples taken during the photoreaction of 0.075 mM 4-nitrophenol alkaline solution; (C) the variation of 4-nitrophenol concentration by photocatalytic reaction with the F-doped TiO_2 nanofilm (S3) and P-25; (D) pseudo-first order kinetic rate plots for the photo-oxidation of 4-nitrophenol.

late TiO_2 thin films. Fig. 8A and B presents the *in situ* kinetics UV–vis spectra recorded at 30-min intervals during the photodegradation of 4-NPh on the F-doped particulate TiO_2 thin film (S3) and the P-25 TiO_2 film under ~2 mW/cm^2 UV and visible irradiation, respectively. Six hundred millivolts versus Ag/AgCl was applied as the anodic bias. The main absorption band centered at ~400 nm significantly decreased with the UV irradiation time. The changes in the concentration of 4-NPh under UV and visible irradiation are shown in Fig. 8C. As the data points after 2-h photodegradation of 4-NPh on S3 are slightly off the line, the corresponding plots ln c/c_0 versus t for the first 2 h were plotted in Fig. 8D. The linear relationship of ln c/c_0 versus t shows that the photocatalytic degradation of 4-NPh follows pseudo-first order kinetics

$$\ln\frac{c}{c_0} = -kt \quad (3)$$

where c/c_0 is the normalized 4-NPh concentration, t the reaction time, and k is the reaction rate in term of min^{-1}. As shown in Fig. 8D, the photodegradation rate constant for the F-doped particulate TiO_2 thin film (S3) is 8.14×10^{-3} min^{-1}, two times higher than that for the P-25 film, 4.10×10^{-3} min^{-1}, further confirming that the F-doped TiO_2 nanoparticulate thin films directly grown on the Ti substrate exhibit superb photocatalytic efficiency for promising environmental applications in the photodegradation of organic pollutants.

4. Conclusions

In summary, we have developed a novel and facile approach to directly grow F-doped TiO_2 particulate thin films with superb visible light photoelectrical response and high photocatalytic efficiency by oxidizing titanium substrate in the presence of H_2O vapor assisted with NaF at relatively low temperatures. Our study has shown that temperature and the amounts of the NaF coated on the Ti substrate significantly affect the morphology and photocatalytic activity of the formed nanoparticulate thin films. The photocurrents of the as-prepared F-doped TiO_2 nanoparticulate thin films are much higher than that of a P-25 TiO_2 film. For instance, the photocurrent at 600 mV for the F-doped TiO_2 thin film prepared at 600 °C and coated with 50 μmol NaF is over seven times higher than that of the P-25 TiO_2 film. In addition, the rate of photodegradation of 4-nitrophenol on the formed F-doped TiO_2 thin film is over two times higher than that on the P-25 thin film. The approach described here can be easily commercialized to fabricate F-doped TiO_2 particulate thin films on a large-scale for very promising environmental applications in wastewater treatment and the photoinduced splitting of water into hydrogen, a *green* energy source.

Acknowledgments

This work was supported by a discovery grant from the Natural Sciences and Engineering Research Council of Canada (NSERC). A. Chen acknowledges the Canada Foundation of Innovation (CFI) and NSERC for a Canada Research Chair Award.

References

[1] M.R. Hoffmann, S.T. Martin, W.Y. Choi, D.W. Bahnemann, Chem. Rev. 95 (1995) 69–96.
[2] L.C. Macedo, D.A.M. Zaia, G.J. Moore, H. Santana de, J. Photochem. Photobiol. A 185 (2007) 86–93.
[3] G. Colon, J.M. Sanchez-Espana, M.C. Hidalgo, J.A. Navio, J. Photochem. Photobiol. A 179 (2006) 20–27.
[4] M.A. Fox, M.T. Dulay, Chem. Rev. 93 (1993) 341–357.
[5] M. Fujihira, Y. Satoh, T. Osa, Nature 293 (1981) 206–207.
[6] B. Sun, E.P. Reedy, P.G. Smirniotis, Environ. Sci. Technol. 239 (2005) 6251–6259.
[7] P.A.M. Hotsenpiller, J.D. Bolt, W.E. Farneth, J.B. Lowekamp, G.S. Rohrer, J. Phys. Chem. B 102 (1998) 3216–3226.
[8] F. Gruy, M. Pijolat, J. Am. Ceram. Soc. 75 (1992) 657–659.
[9] G.R. Yi, J.H. Moon, S.M. Yang, Chem. Mater. 13 (2001) 2613–2618.
[10] S. Nakade, Y. Saito, W. Kubo, T. Kitamura, Y. Wada, S. Yanagida, J. Phys. Chem. B 107 (2003) 8607–8611.
[11] B. Wen, C. Liu, Y. Liu, J. Phys. Chem. B 109 (2005) 12372–12375.
[12] X.S. Peng, A. Chen, Adv. Funct. Mater. 16 (2006) 1355–1362.
[13] J.M. Macak, H. Tsuchiya, L. Taveira, S. Aldabergerova, P. Schmuki, Angew. Chem. Int. Ed. 44 (2005) 7463–7465.
[14] K. Shankar, K.C. Tep, G.K. Mor, C.A. Grimes, J. Phys. D: Appl. Phys. 39 (2006) 2361–2366.
[15] J.H. Park, S. Kim, A.J. Bard, Nano Lett. 6 (2006) 24–28.
[16] X.C. Wang, J.C. Yu, Y.L. Chen, L. Wu, X.Z. Fu, Environ. Sci. Technol. 40 (2006) 2369–2374.
[17] F.H. Tian, C.B. Liu, J. Phys. Chem. B 110 (2006) 17866–17871.
[18] X.L. Yan, T. Ohno, K. Nishijima, R. Abe, B. Ohtani, Chem. Phys. Lett. 429 (2006) 606–610.
[19] J.C. Yu, J. Yu, W. Ho, Z. Jiang, L. Zhang, Chem. Mater. 14 (2002) 3808–3816.
[20] M. Anpo, M. Takeuchi, J. Catal. 216 (2003) 505–516.
[21] C.G. Wu, C.C. Chao, F.T. Kuo, Catal. Today 97 (2004) 103–112.
[22] S. Rodrigues, K.T. Ranjit, S. Uma, I.N. Martyanov, K.J. Klabunde, Adv. Mater. 17 (2005) 2467–2471.
[23] P.N. Kapoor, S. Uma, S. Rodriguez, K.J. Klabunde, J. Mol. Catal. A 229 (2005) 145–150.
[24] W.Y. Choi, A. Termin, M.R. Hoffmann, J. Phys. Chem. 98 (1994) 13669–13679.
[25] W.Y. Teoha, R. Amala, L. Mädlerb, S.E. Pratsinis, Catal. Today 120 (2007) 203–213.
[26] K. Vinodgopal, S. Hotchandani, P.V. Kamat, J. Phys. Chem. 97 (1993) 9040–9044.
[27] A. Lotnik, S. Senz, D. Hesse, Thin Solid Film 26 (2007) 3439–3447.
[28] T. Izumi, T. Teraji, T. Ito, J. Cryst. Growth 299 (2007) 349–357.
[29] N. Arimitsu, A. Nakajima, K. Saito, Y. Kameshima, K. Okada, Chem. Lett. 36 (2007) 106–107.
[30] X. Peng, J. Wang, D.F. Thomas, A. Chen, Nanotechnology 16 (2005) 2389–2396.
[31] J.M. Macak, H. Tsuchiya, P. Schmuki, Angew. Chem. Int. Ed. 44 (2005) 2100–2102.
[32] R. Memming, Top. Curr. Chem. 143 (1988) 81–88.
[33] D. Li, H. Haneda, N.K. Labhsetwar, S. Hishita, N. Ohashi, Chem. Phys. Lett. 401 (2005) 579–584.
[34] N. Serpone, J. Phys. Chem. B 110 (2006) 24287–24293.